RESEARCH ARTICLE

# Expression of Gls and Gls2 Glutaminase Isoforms in Astrocytes

Carolina Cardona,[1,2] Elisabeth Sánchez-Mejías,[2,3,4] José C. Dávila,[2,3,4] Mercedes Martín-Rufián,[5] José A. Campos-Sandoval,[1,2] Javier Vitorica,[4,6,7] Francisco J. Alonso,[1,2] José M. Matés,[1,2] Juan A. Segura,[1,2] Michael D. Norenberg,[8] Kakulavarapu V. Rama Rao,[8] Arumugan R. Jayakumar,[8] Antonia Gutiérrez,[2,3,4] and Javier Márquez[1,2]

The expression of glutaminase in glial cells has been a controversial issue and matter of debate for many years. Actually, glutaminase is essentially considered as a neuronal marker in brain. Astrocytes are endowed with efficient and high capacity transport systems to recapture synaptic glutamate which seems to be consistent with the absence of glutaminase in these glial cells. In this work, a comprehensive study was devised to elucidate expression of glutaminase in neuroglia and, more concretely, in astrocytes. Immunocytochemistry in rat and human brain tissues employing isoform-specific antibodies revealed expression of both Gls and Gls2 glutaminase isozymes in glutamatergic and GABAergic neuronal populations as well as in astrocytes. Nevertheless, there was a different subcellular distribution: Gls isoform was always present in mitochondria while Gls2 appeared in two different locations, mitochondria and nucleus. Confocal microscopy and double immunofluorescence labeling in cultured astrocytes confirmed the same pattern previously seen in brain tissue samples. Astrocytic glutaminase expression was also assessed at the mRNA level, real-time quantitative RT-PCR detected transcripts of four glutaminase isozymes but with marked differences on their absolute copy number: the predominance of Gls isoforms over Gls2 transcripts was remarkable (ratio of 144:1). Finally, we proved that astrocytic glutaminase proteins possess enzymatic activity by *in situ* activity staining: concrete populations of astrocytes were labeled in the cortex, cerebellum and hippocampus of rat brain demonstrating functional catalytic activity. These results are relevant for the stoichiometry of the Glu/Gln cycle at the tripartite synapse and suggest novel functions for these classical metabolic enzymes.

GLIA 2014;00:000–000

**Key words:** glutaminase, astrocytes, glial cells, mitochondrion, nucleus, glutamine, glutamate

## Introduction

Glial cells (neuroglia) have been traditionally considered as cellular scaffolds and supportive elements of neurons in the central nervous system (CNS). However, in the last two decades an overwhelming number of crucial and unexpected findings have dramatically changed this perception for glial cells, particularly for astrocytes which are intimately associated with synapsis. Although astrocytes are electrically unexcitable cells, they can respond to neurotransmission, participate in its regulation as well as in the development and maintenance of synapses (Araque et al., 1998, 2000; Auld and Robitaille, 2003). In fact, the term tripartite synapse was proposed to include this bidirectional communication between astrocytes and neurons into the classical models of synaptic transmission

View this article online at wileyonlinelibrary.com. DOI: 10.1002/glia.22758

Published online Month 00, 2014 in Wiley Online Library (wileyonlinelibrary.com). Received Aug 20, 2014, Accepted for publication Sep 24, 2014.

Address correspondence to J. Márquez, Dept. Biología Molecular y Bioquímica, Facultad de Ciencias, Campus de Teatinos, Universidad de Málaga, 29071-Málaga, Spain. E-mail: marquez@uma.es or A. Gutiérrez, Dept. Biología Celular, Genética y Fisiología, Facultad de Ciencias, Campus de Teatinos, Universidad de Málaga, 29071-Málaga, Spain. E-mail: agutierrez@uma.es

From the [1]Canceromics Lab. Facultad de Ciencias, Departamento de Biología Molecular y Bioquímica, Universidad de Málaga, 29071, Málaga, Spain; [2]Instituto de Investigación Biomédica de Málaga (IBIMA), Málaga, Spain; [3]Departamento de Biología Celular, Genética y Fisiología. Facultad de Ciencias, Universidad de Málaga, 29071, Málaga, Spain; [4]Centro de Investigación Biomédica en Red sobre Enfermedades Neurodegenerativas (CIBERNED), Madrid, Spain; [5]Proteomics Lab, Central Facility Core, University of Málaga, 29071, Málaga, Spain; [6]Departamento de Bioquímica y Biología Molecular, Facultad de Farmacia, Universidad de Sevilla, 41013, Seville, Spain; [7]Instituto de Biomedicina de Sevilla (IBIS)-Hospital Universitario Virgen del Rocío/CSIC/Universidad de Sevilla, Seville, Spain; [8]Department of Pathology, University of Miami Miller School of Medicine, 016960, Miami, 33101, FL.

Additional Supporting Information may be found in the online version of this article.

 

(Araque et al., 1999; Perea et al., 2009). Besides the active roles of astrocytes regulating information transfer between neurons, they also take part in all essential CNS functions: synaptic plasticity and neurogenesis (Alvarez-Buylla et al., 2001), synaptic integrity and synaptogenesis (Jayakumar et al., 2014), control of brain blood flow (Attwell et al., 2010), immunological defense (Barcia et al., 2013), and metabolic and energy homeostasis (Pellerin and Magistreti, 1994, Danbolt, 2001, Magistretti, 2006). Futhermore, Nedergaard and co-worker has recently discovered a novel function mediated by astrocytes: the so-called "glymphatic system," a brain-wide paravascular pathway for cerebrospinal fluid (CSF) and interstitial fluid (ISF) exchange to facilitate efficient clearance of solutes and waste, is supported by water movement through astrocytic aquaporin-4 (AQP4) (Iliff et al., 2013). Taking into account all these emerging roles, it is not surprising that astrocytes have been suggested to contribute to both initiation and propagation of many (if not all) neurological diseases (Verkhratsky et al., 2012).

Glutaminase (GA; EC 3.5.1.2) catalyzes the hydrolytic deamidation of glutamine (Gln) yielding stoichiometric amounts of glutamate (Glu) and ammonium ions. A plethora of experimental evidences from physiological, biochemical, immunological, and nuclear magnetic resonance (NMR) spectroscopic data indicate that biosynthesis of transmitter Glu from Gln through GA is the prevailing pathway for excitatory Glu production (Hertz, 2004; Nicklas et al., 1987). Mammalian glutaminases are encoded by two paralogous genes, *Gls* and *Gls2*, located in distinct chromosomes (Aledo et al., 2000). Two GLS isoenzymes named KGA and GAC, traditionally known as kidney or K-type isoenzymes (see Matés et al., 2013 for an update on GA nomenclature), are derived from the *Gls* gene by alternative splicing (Elgadi et al., 1999; Porter et al., 2002). The *Gls2* gene codes for two additional GLS2 isoenzymes, GAB and LGA (formerly known as liver or L-type isoforms), by using an alternative transcription start site (Martín-Rufián et al., 2012). Experimental evidence supporting GAB as a novel GLS2 isoform, different from the classical LGA liver isozyme, has recently been published (de la Rosa et al., 2009; Martín-Rufián et al., 2012). GLS2 transcripts derived from the *Gls2* gene were initially thought to be present in adult liver tissue and absent in extrahepatic tissues (Curthoys and Watford, 1995). This restricted pattern of expression was recently changed by novel data which demonstrated GLS2 expression in extrahepatic tissues such as brain, pancreas, and breast cancer cells (Gómez-Fabre et al., 2000). Simultaneous expression of GLS and GLS2 transcripts was demonstrated in the brain of human, cow, mouse, rat, and rabbit (Aledo et al., 2000; Gómez-Fabre et al., 2000) and lately confirmed, at the protein level, by biochemical and immunohistochemical approaches (Olalla et al., 2002).

The prevalent and currently accepted view about GA expression in mammalian brain states that GAs are almost exclusively confined in neuronal cells and show a limited or no expression in glial cells, with only a few exceptions: *in vitro* cultured astrocytes, where efficient Gln uptake and GA activity were previously reported (Kvamme et al., 1982; Schousboe et al., 1979), and activated microglia cells that produce Glu in an autocrine manner through up-regulation of GA expression (Takeuchi et al., 2006). In this study, regional, cellular and subcellular distribution, and enzyme activity for GLS and GLS2 isoforms were investigated in brain tissue and cultured astrocytes. A goal was to establish cell-type-specific expression to elucidate novel cerebral functions of GA isoenzymes. We demonstrate expression of GLS and GLS2 isoforms in glutamatergic and GABAergic neurons and astroglial cells by a combination of complementary approaches, including immunocytochemistry/immunofluorescence/electron microscopy (EM) with isoform-specific antibodies, real-time quantitative RT-PCR and *in situ* activity staining to check *in vivo* GA activity. Both GLS (KGA) and GLS2 (GAB/LGA) isozymes were found to be expressed in cerebral cortex, cerebellar, and hippocampal astrocytes. Furthermore, a clear segregation was found for each GA isoform, with KGA appearing only in astrocytic mitochondria while GAB/LGA was preferentially detected in both nucleus and mitochondria.

*Abbreviations*

| | |
|---|---|
| BSA | bovine serum albumin |
| DABCO | 1,4-diazabicyclo [2,2,2] octane |
| DAPI | 4′,6-diamidino-2-phenylindole |
| EM | electron microscopy |
| GA | phosphate-activated glutaminase |
| GAB | *Gls2*-encoded long transcript glutaminase variant |
| GAC | *Gls*-encoded alternative-spliced short transcript glutaminase variant |
| GIP | glutaminase-interacting protein |
| IMAC | immobilized metal affinity chromatography |
| KGA | *Gls*-encoded long transcript glutaminase variant |
| LGA | *Gls2*-encoded short transcript glutaminase variant |
| PBS | phosphate-buffered saline |
| PDZ | postsynaptic density protein PSD-95/SAP90, *Drosophila* tumor suppressor protein DLG, and tight junction protein ZO-1. |

## Materials and Methods

### Brain Tissue and Antibodies

Adult male Sprague-Dawley rats ($n = 12$) were obtained from *Charles River Lab* (Barcelona, Spain). For immunohistochemical studies, animals ($n = 8$) were deeply anesthetized and perfused transcardially with phosphate buffer saline (PBS) followed by ice-cold fixative solution (4% paraformaldehyde, 75 mM lysine, and 10 mM sodium metaperiodate). After overnight postfixation in the same fixative, brains were sectioned (50 μm) in a vibrotome (for immunoelectron microscopy studies) or cryoprotected (30% sucrose), frozen and then sectioned (30 μm) in a freezing microtome (for single or

double immunohistochemistry). For GA activity assay, animals ($n = 4$) were sacrificed by decapitation. Brains were quickly removed, frozen in liquid-nitrogen-cooled isopentane and embedded in Tissue-Tek® OCT™ compound (Sakura Finetek Europe, NL) for cryostat sectioning. Sections (20 μm thickness) were picked up onto polylysine-coated glass slides and immediately processed for GA activity histochemical staining. All animal experiments were carried out in accordance with the European Union regulations (Council Directive 86/609/ECC of 24 November 1986) and approved by the committee of animal use for research at Malaga University, Spain (RD 1201/2005 of 10 October 2005).

Human brain tissue was obtained from the *Institute of Neuropathology Brain Bank IDIBELL-Hospital Universitari de Bellvitge* (Barcelona, Spain) at autopsy from individuals ($n = 2$, age range $56 \pm 2$) free of any known neurological or psychiatric illness, with a postmortem delay between 3 and 14 h. The brain samples were obtained with the approval of local ethics committee following Spanish legislation. Samples of the hippocampal cortex were fixed in 4% paraformaldehyde in 0.1 M phosphate buffer (PB) for 24–48 h, cryoprotected in sucrose, stored at −80°C, sectioned (30 μm thickness) on a freezing microtome and serially collected in wells containing 0.1 M PBS and 0.02% sodium azide.

The following antibodies were used in this study: the rabbit polyclonal antibodies anti-KGA and anti-GAB were generated and characterized in our laboratory (Olalla et al., 2002; Campos et al., 2003; Olalla et al., 2008). A second anti-GAB antibody was also raised in rats by using similar protocols and the same antigen employed for rabbit immunization (whole GAB protein sequence). The rat antibody was essentially used to double-check and confirm most immunohistochemical and immunocytochemical results, but usually it showed lower signals than the rabbit antibody. The chicken polyclonal anti-glial fibrillary acidic protein (GFAP) and the mouse monoclonal anti-ATP synthase were from Merck Millipore (Germany). The biotinylated secondary goat anti-rabbit IgG was from Vector Labs (United Kingdom). Alexa Fluor 568/488/405 conjugated donkey anti-mouse, goat anti-rabbit, or goat anti-chicken secondary antibodies (IgG) were from Invitrogen (USA).

### Immunohistochemistry

Procedure was as described previously (Olalla et al., 2002, 2008). Briefly, free floating sections, after blocking the endogenous peroxidase activity, avidin, biotin, and biotin-binding proteins for 30 min with avidin-biotin blocking Kit (Vector Labs, United Kingdom), were incubated with the affinity-purified rabbit polyclonal anti-KGA antibody (1:500; Olalla et al., 2002) or rabbit polyclonal anti-GAB antibody (1:2,000 dilution) for 48 h at room temperature. The tissue-bound primary antibody was then detected by incubating with biotinylated anti-rabbit IgG (Vector Labs, United Kingdom) for 1 h at room temperature (1:500 dilution) and then with ExtrAvidin-peroxidase conjugate (Sigma-Aldrich, Spain) for 1 h at room temperature (1:2,000 dilution). Immunoreaction product was visualized with 0.05% 3-3'-diaminobenzidine tetrahydrochloride (DAB; Sigma-Aldrich, Spain), 0.03% nickel ammonium sulphate, and 0.01% $H_2O_2$ in PBS. Sections were then mounted onto gelatin-coated slides, dehydrated in graded ethanol, cleared in xylene and coverslipped with DPX mounting medium (VWR BDH Prolabo, VWR International). Immunostaining was observed under a Nikon Eclipse 80i microscope and images acquired with a Nikon DS-5M high-resolution digital camera. All immunohistochemical studies by light and electron microscopy were tested using negative controls (omitting the primary antisera) and no immunoreaction products were detected in any case.

### Immunofluorescence and Confocal Microscopy

For double immunofluorescence labelings of KGA/GFAP and GAB/GFAP, free-floating sections were first heated at 80°C for 20 min in 50 mM citrate buffer pH 6.0 for antigen retrieval. After blocking with 5% goat serum (Sigma-Aldrich) in PBS for preventing nonspecific staining, sections were first sequentially incubated with primary antibodies (rabbit anti-KGA, 1:500 dilution, see Olalla et al., 2002; rabbit anti-GAB, 1:1,000 dilution, chicken anti-GFAP, 1:2,000 dilution, Merck Millipore) over 24 or 48 h at room temperature, followed by the corresponding Alexa 568/488 secondary antibodies (1:1,000 dilution, Invitrogen). Sections were then mounted onto gelatin-coated slides, air dried, coverslipped with PBS containing 50% glycerin and examined under a confocal laser microscope (Leica SP5 II). In the case of human brain sections, they were also incubated in *autofluorescence eliminator reagent* (Merck Millipore), following the manufacturer's recommendations, to eliminate fluorescence emitted by intracellular lipofuscin accumulation with age. Specificity of the immune reactions was controlled by omitting the primary antisera and by preadsorption with specific antigens.

### Immunocytochemistry

For triple immunofluorescence labeling of KGA/GFAP/ATP synthase or GAB/GFAP/ATP synthase, coverslips containing cultured mouse astrocytes were fixed with 4% paraformaldehyde in PB, pre-treated with PBS containing 0.1% Triton X-100 for 12 min, blocked with 1% bovine serum albumin (BSA, Sigma Aldrich) in PBS containing 0.1% Triton X-100 for 1 h at room temperature, and sequentially incubated with primaries antibodies (rabbit anti-KGA 1:500 dilution or anti-GAB 1:1,000; mouse anti-ATP synthase, 1:1,000 dilution, Merck Millipore; chicken anti-GFAP, 1:2,000 dilution, Merck Millipore) overnight at 4°C. Cells were then incubated with the corresponding Alexa 568/488/405 secondary antibodies (1:500 dilution, Invitrogen) and coverslips were mounted onto gelatin-coated slides with PBS containing 50% glycerin. Finally, astrocytes were observed under a confocal laser microscope (Leica SP5 II).

### Immunoelectron Microscopy

The KGA immunolabeling method for transmission electron microscopy (TEM) was essentially identical to the described above for immunohistochemistry, except that Triton X-100 was eliminated from all solutions and no nickel ammonium sulphate was added to the DAB solution. After the DAB reaction, the 50 μm vibratome sections from rat brain were washed in PBS, treated with 1% $OsO_4$ in PBS for 1 h, dehydrated in acetone, and flat-embedded between aluminium sheets in Araldite 502 (EMS, Hatfield, PA, USA). To increase contrast, the sections were treated with 1% uranyl acetate (EMS, Hatfield, PA, USA) in 70% acetone during dehydration.

After a light microscopic examination, selected flat-embedded sections were glued onto prepolymerized resin blocks and cut at 70–80 nm on a Reichert Ultracut E ultramicrotome. Ultrathin sections were collected on copper grids and examined with a Jeol JEM1400 electron microscope.

### Glutaminase In Situ Activity Staining

GA activity was determined on 20 μm cryostat brain section using a tetrazolium salt method (Montero et al., 2007) modified for mammalian brain tissue. Unfixed cryostat sections were allowed to adjust to RT. Then, 100 mL of medium were poured onto sections which were then incubated in darkness for 40 min at 37°C. The incubation medium contained: 3% (w/v) polyvinyl alcohol as tissue protectant; 200 mM Tris/HCl buffer (pH 8.0); 200 mM $KH_2PO_4$; 40 mM Gln; 0.1 mM EDTA; 3.4 mM $NAD^+$; 0.5 mM ADP; 0.3 mM nitroblue tetrazolium (NBT); 0.49 mM phenazine methosulfate (PMS); and 80 units of glutamate dehydrogenase (GDH, EC 1.4.1.2) used as an auxiliary enzyme. Control reactions were always run in parallel where either Gln (the GA substrate) or Pi (an essential activator of GA) was omitted. After incubation, sections were immediately washed at 60°C with 100 mM phosphate buffer (97.5 mM $KH_2PO_4$/2.5 mM $NaH_2PO_4$, pH 5.3) to stop the reaction and remove the incubation medium, postfixed in 4% formaldehyde and mounted in glycerol medium. To identify GA activity in astrocytes cells, after postfixation some sections were processed for immunofluorescence by incubating with anti-GFAP (1:2,000 dilution, Merck Millipore) for 24 h at RT and then 90 min with the corresponding secondary antibody goat anti-chicken Alexa Fluor 568/488 (1:500 dilution, Invitrogen).

### Astrocyte Isolation and Culture

For immunocytochemistry assays, primary astroglial cultures (Saura et al., 2003) were prepared from newborn (1–3 days) C57BL/6 mice. Briefly, dissected brains were treated, for 5 min at 37°C, with trypsin-DMEM-EDTA medium (Biowhittaker, Cambrex). Treatment was stopped using complete DMEM-F12 plus 10% FBS and the cells were mechanically dissociated. After mechanical dissociation, the debris were eliminated by filtration (40 μm; BD Falcon) and the cells were seeded, at a density of 250,000 cells/mL, in DMEM-F12 plus 10% FBS medium (containing glutamine, nonessential amino acids, 1% penicillin-streptomycin and gentamycin) on poly-D-lysine (Sigma-Aldrich)-treated Nunc 12-well plates. The cells were cultured at 37°C, in humidified 5% $CO_2$/95% atmosphere. Medium was replaced every 4 days. After 13–15 days in culture, astroglial cells were isolated by mild trypsinization (0.1%) with nonsupplemented DMEM-F12. After 30 min incubation, the treatment was stopped, using complete medium. Astrocytes were detached as an intact layer in the complete medium. After detachment, astrocytes were isolated by centrifugation, at 800*g* for 5 min, and cultured in complete medium. Using this approach, the microglial contamination (determined using GFAP (astrocyte marker) and Iba-1 (microglial marker)) was lower than 5%.

For real-time qRT-PCR we use cerebellar astrocytes isolated from 0 day postnatal rat brain tissue obtained from a commercial source (Innoprot, Spain). Sprague Dawley rats were subjected to standard diet and lighting circadian cycle (12:12 h). Approximately, $10^6$ cells from rat cerebellum, 0 day postnatal (no verified sex), were isolated by immunomagnetic separation under agreed conditions (incubation time for cleaning of cells not exceeding 24 h and Gln omitted from the stabilizing medium). Isolated rat astrocytes were cryopreserved by frozen in CryoStor CS10 (10% DMSO) at passage one and delivered frozen.

### Real-Time Quantitative RT-PCR

Total RNA from rat cerebellar astrocytes was isolated according to manufacturer's specifications (AllPrep DNA/RNA/Protein Mini Kit, Qiagen). Total RNA (1 μg) were reverse transcribed using the Quantitec Reverse Transcription kit (Qiagen) in a 20 μL reaction, according to manufacturer's instructions. RNA samples were tested for genomic DNA contamination by including reverse transcriptase (RT) omitted controls, and for reagents and aerosol contamination by including two nontemplate controls. Real time PCR was carried out with the CFX thermocycler (Bio-Rad) as described elsewhere (Martín-Rufián et al., 2012). KGA and GAC transcripts were amplified using rat isoform-specific primers: KGA forward (5′ CAGAACAGCCCTGCATGTTGCTG 3′), KGA reverse (5′ CCACCTGT CCTTGGGGAAGGGGT 3′), GAC forward (5′GGCATTCCTTT GGACCATTGGAC3′), and GAC reverse (5′CCTCTCCCCCAGA CTTTCCATTC3′). Primers used for Gls2 transcripts were as described previously (Martín-Rufián et al., 2012). Results were evaluated using CFX Bio-Rad Analysis Software. Amplicon size and the absence of nonspecific products were confirmed by agarose gel electrophoresis. For absolute quantification of GA transcripts, PCR transcript-specific amplicons were prepared as standards. PCR products were analyzed by 2% agarose gel electrophoresis and purified (IllustraTM GFXTMPCR DNA and Gel Band Purification Kit, GE Healthcare). The standard curve was created by plotting the threshold cycle (Ct) corresponding to each standard, versus the value of their corresponding log of starting quantity (DNA copy number). The different GA transcripts were expressed as numbers of molecules (±SEM) of mRNA per ng of total RNA.

### Western Blotting

Animals were killed by decapitation. The brain was immediately isolated, frozen in liquid nitrogen, and stored at −80°C until use. Mitochondria from rat liver and kidney were isolated as previously described (Campos et al., 2003). Lysates of rat brain and liver were homogenized (∼5 mg of tissue were added to ∼300 μL lysis buffer) and incubated in a buffer containing 150 mM sodium chloride, 1.0% Triton X-100 and 50 mM Tris/HCl, pH 8.0 (containing the complete protease inhibitor kit, Roche), for 2 h at 4°C, and then centrifuged at 10,000*g* for 15 min at 4°C. Equivalent amounts of protein extracts (35–40 μg of whole tissue extracts, 10–20 μg of mitochondrial extracts, and 10 ng of purified KGA and GAB recombinant proteins; see Olalla et al., 2002) were loaded and run on 10–15% sodium dodecyl sulfate-polyacrylamide gels electrophoresis (SDS-PAGE) and electroblotted onto nitrocellulose membranes. Membranes were blocked with a blocking buffer containing PBS, 0.1% Tween 20, and 5% BSA (Merck) at RT for 1 h. After blocking, membranes were incubated overnight at 4°C with primary

antibodies anti-KGA (1:1,000 dilution), rat anti-GAB (1:2,000 dilution), and rabbit anti-GAB (1:2,000 dilution). A peroxidase-conjugated goat anti-rabbit/anti-rat (Sigma) was added (1:80,000) for 1 h at RT. Marker proteins with defined molecular masses (MagicMark$^{TM}$ XP Western Protein Standard, Invitrogen) were used for molecular mass determination in immunoblots. Membranes were then subjected to repeated washing in PBS-Tween buffer and specific protein bands visualized using the enhanced chemiluminescence technique (SuperSignal$^{TM}$ West Pico Chemiluminescent Substrate, Thermo Scientific). Control preadsorption tests were performed on immunoblots and brain sections. In both cases, antibodies were diluted in blocking solution to the desired concentrations. Each of these antibody solutions was then divided in 2 aliquots and 150 μg of the antigenic recombinant protein was added to 1 aliquot from each pair. The paired aliquots were then incubated overnight at 4°C.

## Results

### *Regional Expression of GA Isoforms in Rat Brain*

In this work, we first study the regional expression of KGA and GAB isoforms in rat brain in order to confirm and extend previous data on brain GA expression and, at the same time, validate our new set of isoform-specific affinity purified antibodies against human GAs (see "Materials and Methods"). To assess potential cross-reactivity of GAB antisera against KGA and vice versa, we immunoblotted proteins from rat liver, brain and kidney samples as well as the recombinant human proteins GAB and His-KGA$_{551–669}$. The ability to recognize the GAB but not the KGA antigen was used as a criterion to designate a serum as GAB-specific and vice versa (Supp. Info. Fig. 1). Antibodies anti-KGA-(551–669) and anti-GAB-(1–602) were selected for subsequent experiments because they had a higher isoform-specific signal-to-noise ratio than others. In all cases, preadsorption of affinity purified antibodies with the antigenic protein used for their generation completely abolished immunoreactivity, both in Western blots as in immunocytochemical assays. Furthermore, for the KGA antibodies used in this study, an additional proof of specificity was obtained by siRNA knockdown of KGA in human glioblastoma cell lines which caused a nearly complete loss of specific immunoreactivity (Martín-Rufián et al., 2014). Therefore, the antibodies used in this study meet all the relevant criteria previously established for isoform-specific anti-GA antibodies (Olalla et al., 2002, 2008) without showing cross-reactivity at the working dilutions employed (Supp. Info. Fig. 1). Finally, we want to stress that KGA antibodies were raised against a unique C-terminal region of this isoform, which is absent in the GAC isoform, and hence they cannot recognize this second Gls isoform (GAC); however, GAB antibodies would recognize both Gls2 isoforms (GAB and LGA).

The pattern of KGA and GAB immunostaining showed an intense label in the main regions involved in glutamatergic or GABAergic neurotransmission such as cerebral cortex, hippocampus, cerebellum, and striatum (Figs. 1 and 2). In the cortex, there was a clear GAB immunoreactivity in nuclei of numerous neurons that was present in all cortical layers (I–VI) with similar intensity, except for layer I that showed the lowest signal (Fig. 1). In sharp contrast, KGA labeling was revealed in cytoplasm and concentrated in neuronal soma and initial portion of dendrites (Fig. 1). Although KGA staining was seen in all cortical layers, the pyramidal cells of layers V and VI exhibited the highest signals. Most labeled neurons were of pyramidal morphology even though some reactive nonpyramidal neurons were also detected. A punctate pattern of KGA staining was clearly seen in the neuropil of all cortical layers. Examination under higher magnification revealed a cytoplasmic particulate immunoreactivity pattern for the KGA antigen, strongly suggestive of its characteristic mitochondrial localization (Olalla et al., 2002).

In the hippocampus, a strikingly different pattern for GAB and KGA isozymes was also revealed (Fig. 1). GAB immunoreactivity was concentrated in neuronal nuclei of most cells of the pyramidal layer in the CA regions and rest of the hippocampal formation including SR, SLM and SO layers. In the dentate gyrus, GAB labeling was detected in the nucleoplasm of cells from the granular and molecular layer and hilus (h) region (Fig. 1). The KGA isoform showed a more intense expression in the pyramidal neurons of the CA3 subfield (pyramidal layer) and lower staining in the CA2 and CA1 regions (Fig. 1). Hippocampal neurons from the hilus expressed KGA as well. This differential pattern of GA immunoreactivity for GAB and KGA was also observed in rat cerebellum. Strong nuclear immunoreactivity for GAB was detected in cells from all layers of the cerebellar cortex, including granule cells, Purkinje cells, and inhibitory GABAergic neurons of the molecular layer (Fig. 2). Cytoplasmic KGA staining was revealed in granular glutamatergic cells, Purkinje cells and GABAergic neurons from the molecular layer (Fig. 2). Finally, in the striatum, we also observed the nuclear staining for GAB and a prevalent KGA immunolabeling in the neuropil with its typical punctate appearance (Fig. 2).

### *Expression of Gls Isoform KGA in Astrocytes from Rat and Human Brain Tissue*

Once the regional expression of GA isoforms was established in rat brain by using isoform-specific antibodies, we focused on glial cells examining the isoform-specificity of GA. In order to confirm the presence of both GA isoforms, and to carry out a comparative study of the cellular and subcellular localization of these isoenzymes, we focused on the astrocyte populations of two main brain regions: cerebral cortex and hippocampus. Electron microscopic immunocytochemistry

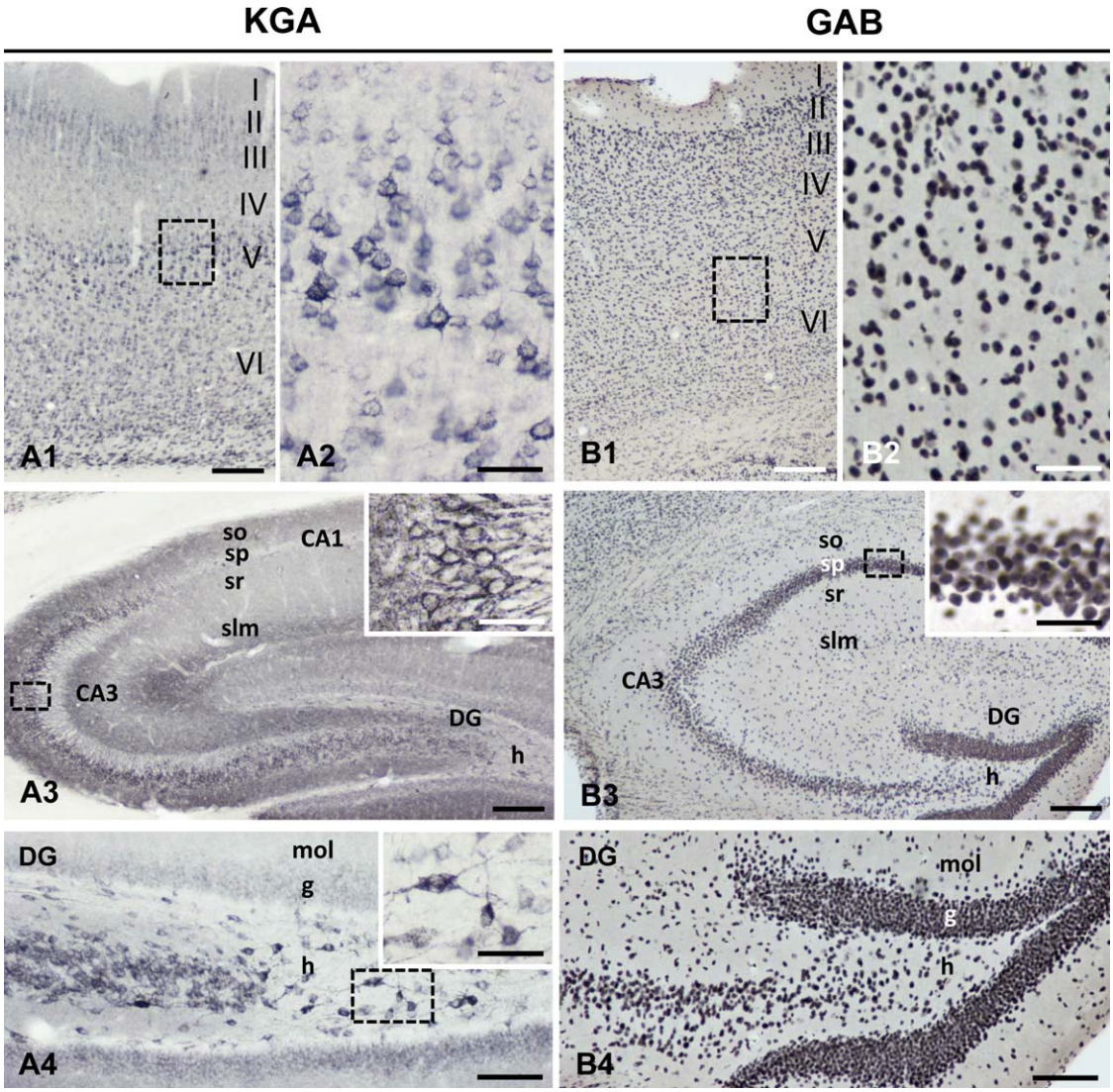


**FIGURE 1: KGA and GAB in rat cerebral cortex and hippocampus. Immunohistochemistry with GA isoform-specific antibodies reveals cytoplasmic KGA (A1–A4) and nuclear GAB (B1–B4) labeling in cerebral cortex (A1–A2 and B1–B2) and hippocampus (A3–A4 and B3–B4). Cortical layers V and VI (A1 and detailed image in A2), CA3 pyramidal neurons (A3 and inset) and dentate gyrus hilar neurons (A4 and inset) exhibited the highest labeling for KGA antibody. GAB pattern was homogeneous within cortical (B1 and detail in B2) or hippocampal layers (B3 and inset, B4). I–VI, cortical layers; CA1–CA3 hippocampal subfields; DG, dentage gyrus; g, granular layer; h, hilus; mol, molecular layer; so, stratum oriens; sp, stratum pyramidale; sr, stratum radiatum; slm, stratum lacunosum moleculare. Scale bars: 200 μm (A1, B1 and A3, B3); 100μm (A4 and B4); Insets 50 μm. [Color figure can be viewed in the online issue, which is available at wileyonlinelibrary.com.]**

demonstrated the presence of KGA in astrocytes (Fig. 3A–D) while confirmed the previously established KGA staining in neurons (Fig. 3G–H). The ultrastructural study in rat hippocampus clearly demonstrated a mitochondrial location of KGA in astrocytes; this immunostaining in glial cells was very similar to that shown by neurons. However, the abundance of mitochondrial labeling in neurons (Fig. 3G) was considerably higher than in astrocytes, where only a discrete number of mitochondria showed KGA reactivity (Fig. 3D). The technique allowed determination of the astrocytic nuclei (Fig. 3A) along with low-dense cytoplasm showing intermediate filaments typical from astrocytes (Fig. 3B).

The antibodies developed against the human KGA enzyme yielded a weak signal in rat astrocytes by immunohistochemistry with DAB-Ni or by immunofluorescence (data not shown). Therefore, we used postmortem human brain tissue for immunohistochemical assays to detect KGA in astrocytes. In human tissue, there was a strong signal in astrocytes from hippocampus and cerebral cortex from the temporal lobe (Fig. 4). Examination by laser scanning confocal microscopy, after double immunofluorescence labeling with anti-KGA and anti-GFAP antibodies, revealed a cytoplasmic particulate immunoreactivity pattern for the KGA antigen, strongly suggestive of a mitochondrial localization (Fig. 4A–C). Such mitochondrial localization of KGA in astrocytes is

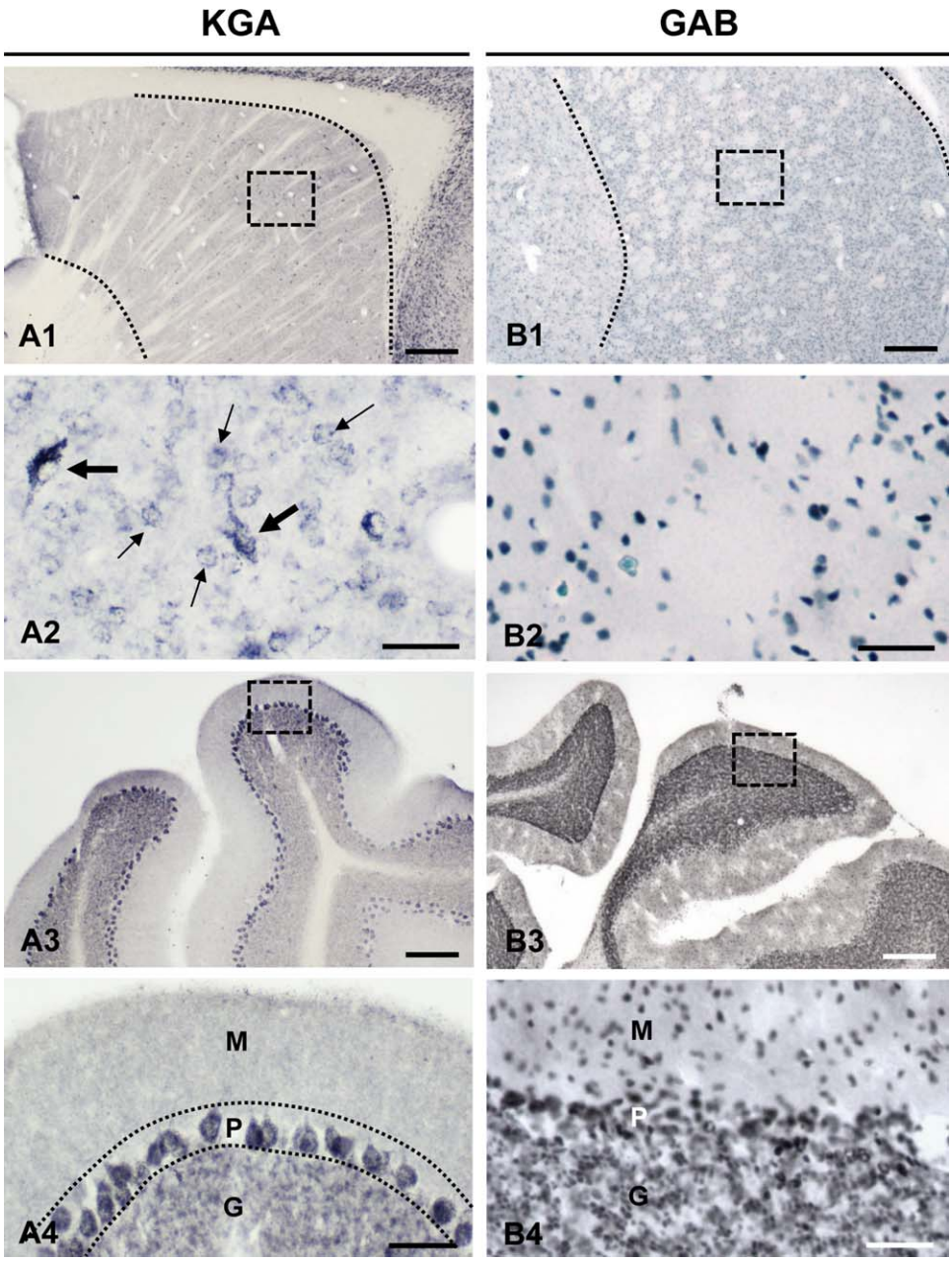


**FIGURE 2: KGA and GBA in the rat striatum and cerebellum. Immunohistochemistry reveals cytoplasmic KGA labeling (A1–A4) and nuclear GAB labeling (B1–B4) in striatum (A1–A2 and B1–B2) and cerebellum (A3–A4 and B3–B4). In striatum, KGA antibody labeled medium-sized projection neurons (A2 thin arrows) and large-sized interneurons (A2 thick arrows). In cerebellum, KGA staining was intense in Punkinje and granular cell layers. GAB immunostaining was detected in cellular nuclei throughout striatum and cerebellar layers. M, molecular layer; P, Purkinje cell layer; G, granular cell layer. Scale bars: 400 μm (A1 and B1); 200 μm (A3 and B3); 50 μm (A2, B2, A4 and B4). [Color figure can be viewed in the online issue, which is available at wileyonlinelibrary.com.]**

complementary with the results obtained by electron microscopy in rat brain (Fig. 3). As expected, neuronal somata and primary dendrites were also abundantly stained (Fig. 4).

### *Expression of Gls2 Isoform GAB in Astrocytes from Rat Brain Tissue*

In sharp contrast with the mitochondrial localization of KGA found in astrocytes, the *Gls2*-encoded GAB isoform was essentially concentrated in astrocytic nuclei (Fig. 5). Double immunofluorescence labeling for GAB and GFAP showed that most GAB immunoreactivity was revealed in the cell nucleus of rat hippocampal astrocytes, although some astrocytic processes were also stained with a cytoplasmic mark (Fig. 5, open arrows). GAB was present in nuclei and specialized foot-processes (white arrows in Fig. 5-C2) of perivascular astrocytes (Fig. 5-C3). A further GAB nuclear mark was also

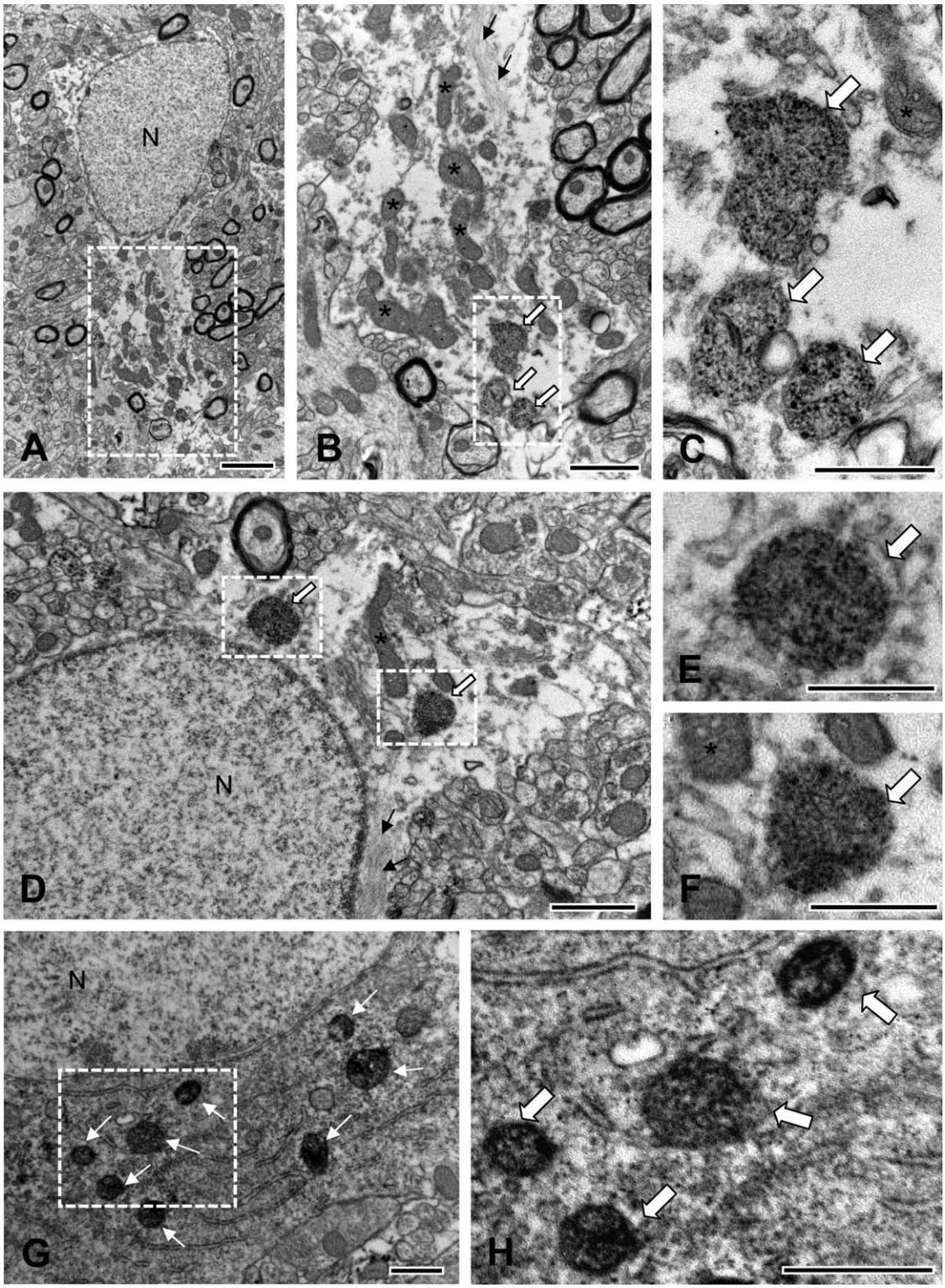


FIGURE 3: Immunoelectron microscopy detection of KGA in the mitocondria of rat brain astrocytes. KGA labeling was restricted to the mitochondria in astrocytes (**A–F**), as seen in neurons (**G–H**), in accordance with the mitochondrial localization of this protein. B and C are higher magnification images from the astrocyte in A showing the immunoreactive cytoplasm and mitochondria (white arrows). E and F are details of some immunopositive mitochondria (white arrows) from the astrocyte in D. Astrocytes were ultrastructurally identified by their low electrodensity cytoplasm and the presence of gliofilaments (black arrows in B and D). Asterisks in B indicate mitochondria that were immunonegative for KGA in astrocytes. N, nuclei. Scale bars: 2 μm (A); 1 μm (B and D); 0.5 μm (C, E, F, and H).

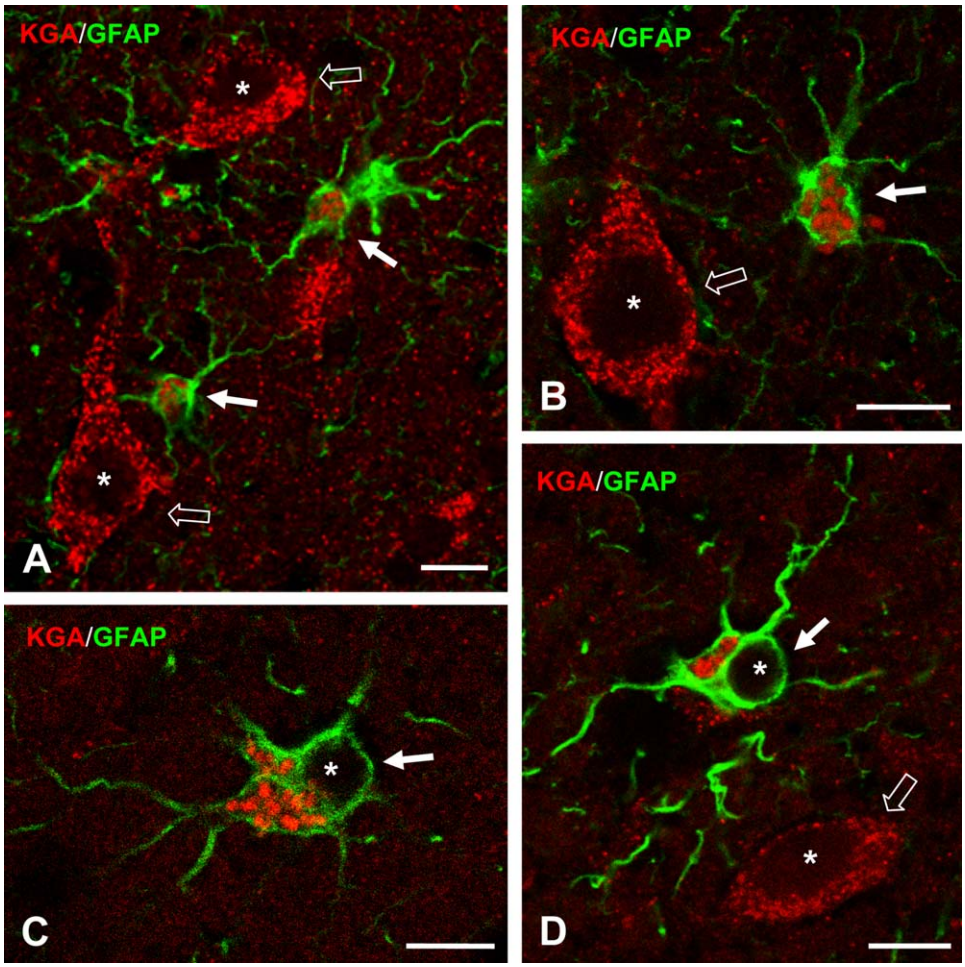


**FIGURE 4: KGA in human brain astrocytes. (A–D) Double immunofluorescence for KGA (red) and GFAP (green) in human brain temporal lobe sections. Punctate KGA immunostaining is clearly seen in the cytoplasm of neurons (open arrows) and astrocytes (white arrows). Asterisks (*) indicate the nuclei of neurons and astrocytes. Images were taken by confocal laser scanning microscopy of human brain sections. Scale bars: 10 μm. [Color figure can be viewed in the online issue, which is available at wileyonlinelibrary.com.]**

detected in GFAP-negative cells (Fig. 5-A3, open arrows) and probably corresponds to neuronal nuclei, a location previously reported for GAB in mammalian brain (Olalla et al., 2002).

### *Expression of Gls and Gls2 Isoforms in Cultured Astrocytes*

The results of astrocyte GA expression obtained in human and rat brain tissues were validated by using mouse cultured astrocytes. Triple immunofluorescence labeling with isoform-specific GA antibodies, anti-ATP synthase (mitochondrial marker) and anti-GFAP (astrocyte marker) employing laser scanning confocal microscopy confirmed the subcellular locations for KGA and GAB isoforms. Thus, the KGA immunoreactivity mimics that of mitochondrial ATP synthase (Fig. 6), reinforcing the exclusive mitochondrial location previously revealed for this Gls isoform in rat and human brain tissue (Figs. 3 and 4). In contrast, the triple immunofluorescence labeling for GAB/ATP synthase/GFAP revealed a clear nuclear localization of GAB, along with an intense mitochondrial staining fully overlapping the ATP synthase signal (Fig. 6). The nuclear location of GAB in cultured astrocytes supports the results previously seen using fresh brain tissue preparations, whereas the profuse mitochondrial label shown by *in vitro* cell cultures was considerably stronger than that of brain sections (where GAB was mostly confined in astrocytic nuclei) and might be related to culture conditions (see discussion section). In any case, these results dealing with cultured astrocytes using cell- and organelle-specific antibodies and confocal microscopy strongly reinforced the results obtained *in situ* with rat and human brain tissue.

### *Astrocyte GA is a Functional Enzyme*

We next investigated whether glial GA is a catalytically active enzyme, because immunoassays with isoform-specific antibodies do not warrant a fully functional enzyme being operative in these brain cells. For this purpose, we set up an *in situ* activity staining originally devised to detect GA activity in

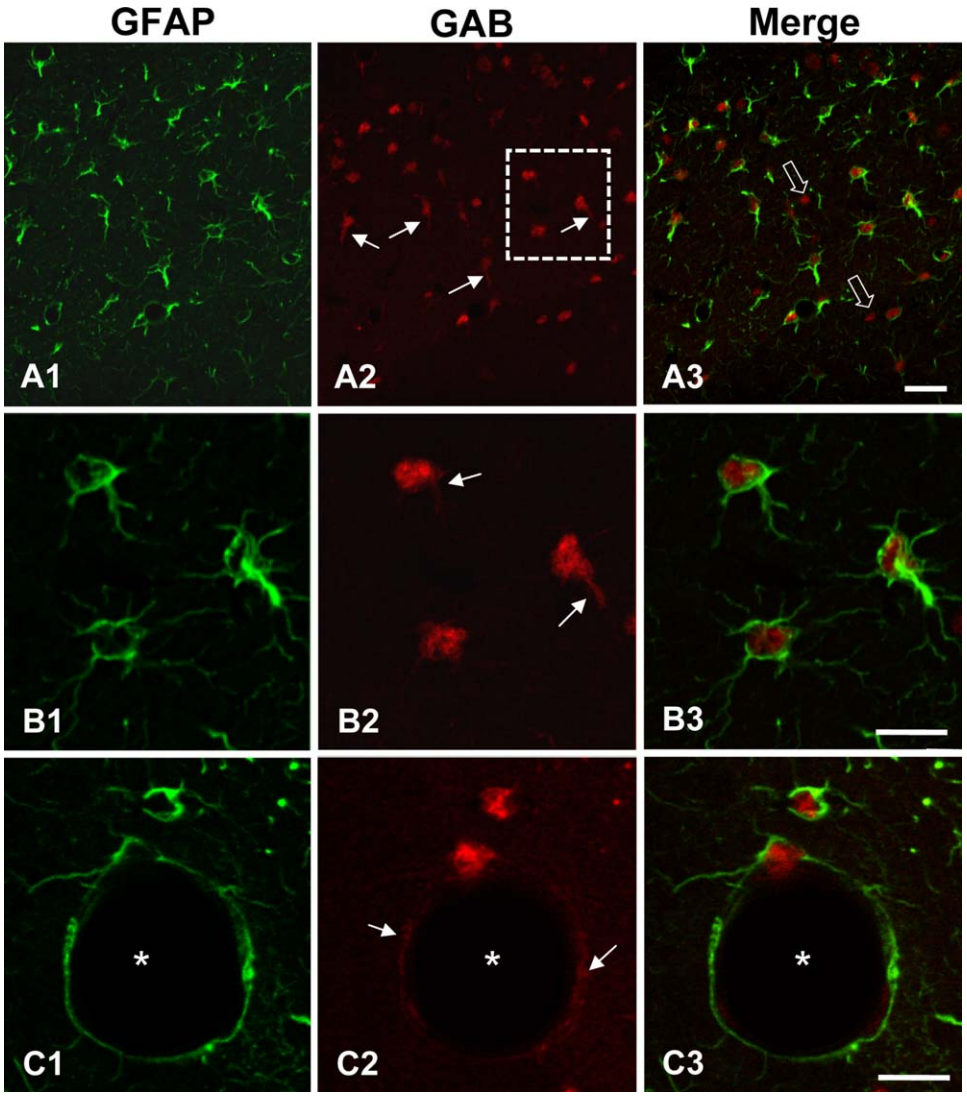


**FIGURE 5: GAB in rat brain astrocytes. Confocal microscopy and double immunofluorescence for GFAP (green; A1–C1) and GAB (red; A2–C2) in rat hippocampus. Merge images (A3–C3) show the location of GAB in the nuclei and processes (white arrows in A2 and B2) of rat astrocytes. GAB is also present in nuclei and specialized foot-processes (white arrows in C2) of perivascular astrocytes (C3). Open arrows in A3 indicate GFAP-negative cells with GAB-positive nuclei. Asterisk indicates a blood vessel. Scale bars: 50 μm (A) and 20 μm (B, C). [Color figure can be viewed in the online issue, which is available at wileyonlinelibrary.com.]**

native electrophoresis gels (Aledo et al., 1993), lately adapted to immunohistochemical detection of GA in pancreas (Montero et al., 2007) and now modified for rat brain tissue. The assay was first optimized for substrate and activator concentrations, incubation times, and the amount of GDH used as an auxiliary enzyme. The dark-blue stain of the NBT-formazan produced was easily detected in rat cortex and cerebellum, while no significant staining was seen when either the substrate (Gln) or the activator (Pi) were omitted as negative controls of the assay (Fig. 7D1–D2). In cerebellum, the highest GA activity was seen in the granular layer and Purkinje cells, along with an intense mark in the Bergmann glia; in contrast, no significant activity was detected in the molecular layer of the cerebellum (Fig. 7C1–C2). In rat hippocampus, GA activity was revealed in the cytoplasm of neurons of the granular layer, resembling the punctate aspect characteristic of its mitochondrial location (Fig. 7A1–A3), while in cerebral cortex the staining was intense and broadly distributed by all cortical layers (Fig. 7B1–B2). Furthermore, we did not detect GA activity in any cell nuclei of the different regions examined (Fig. 7).

Once the *in situ* activity assay was optimized in fresh brain sections, we examined for astrocytic reactivity by using the GFAP immunolabeling immediately after finishing the GA assay. We were able to detect *in vivo* astrocyte GA activity in cerebellum and cortex (Fig. 8), despite of the presence of an intense background due to neuronal GA activity. A discrete population of astrocytes containing GA activity was

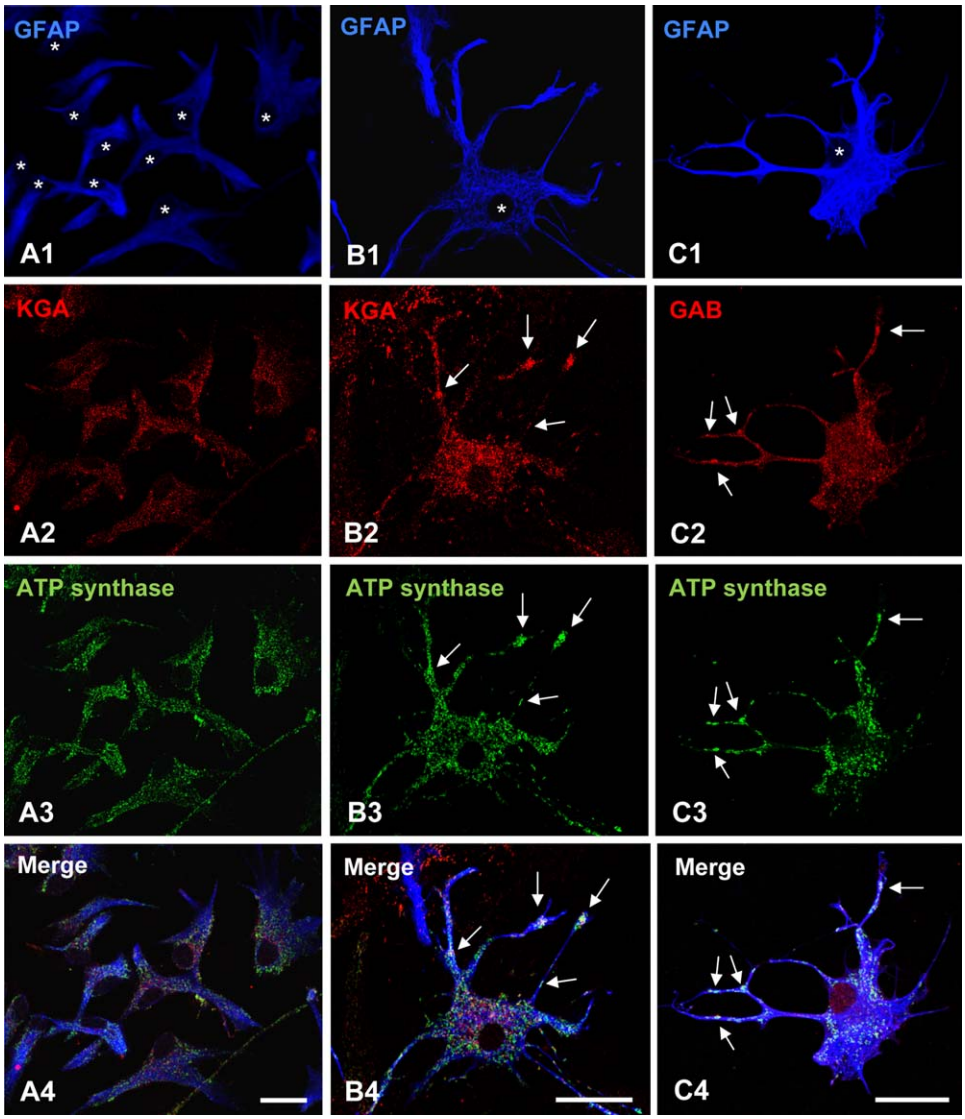


**FIGURE 6: KGA and GAB glutaminases in cultured astrocytes. Confocal microscopy of triple immunofluorescence staining for GFAP (A1–C1), KGA (A2 and B2) or GAB (C2) isoforms and ATP synthase (A3–C3) in primary astroglial cultures from mice brain. Merge images show colocalization of KGA with the mitocondrial marker ATP synthase (arrows in B4) whereas GAB is present in both mitochondria (arrows in C4) and nucleus. Asterisks in A1–C1 indicate the nuclear region of astrocytes. Scale bar: 25 μm in all panels. [Color figure can be viewed in the online issue, which is available at wileyonlinelibrary.com.]**

identified, although many glial cells did not show the blue formazan precipitate which indicates the presence of a functional GA activity. The granular or punctate appearance of the staining in GA-positive astrocytes resembles the KGA immunoreactivity suggesting a mitochondrial location.

### *Quantitative mRNA Levels of GA Isoforms in Rat Astrocytes*

Finally, we addressed the identification and quantitation of GA transcripts expressed by rat astrocytes. A real-time RT-PCR (qRT-PCR) method was devised targeting the four GA isoforms so far reported to be expressed in mammalian tissues (Márquez et al., 2010; Martín-Rufián et al., 2012). Total RNA was extracted from astrocytes isolated from rat cerebellum, a region where we found a significant population of cells positive for GA activity staining. The total copy number (normalized vs. the amount of total RNA) of four GA isoforms: KGA, GAC, GAB, and LGA, are depicted in Fig. 9. A striking result was the strong prevalence shown by Gls transcripts (KGA+GAC) vs. Gls2 (GAB+LGA) ones: >99% of total astrocytic GA mRNA belong to transcripts encoded by the *Gls* gene. The most abundant Gls transcript variant was GAC, with a copy number value double of the KGA isoform ($572.133 \pm 86.37$ vs. $292.133 \pm 45.95$) (Fig. 9). With regard to Gls2 transcript variants, the long isoform GAB was predominant and displayed a copy number about 10-fold bigger than the value shown by short variant LGA, which appears scarcely transcribed in cerebellar astrocytes ($0.652 \pm 0.197$).

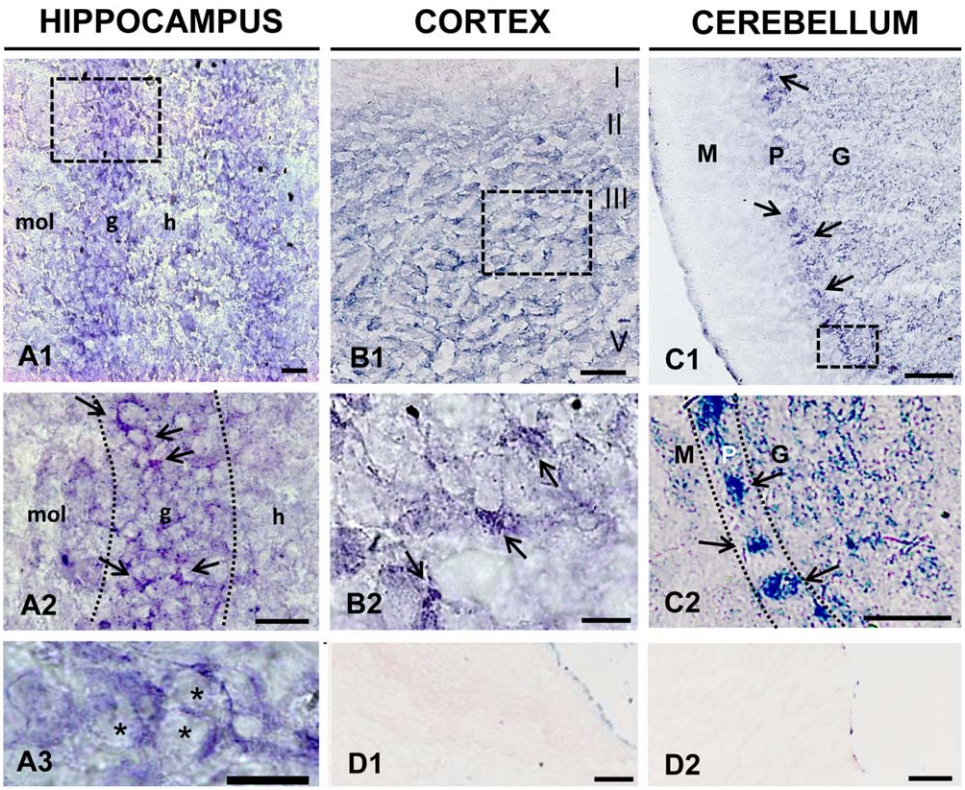


**FIGURE 7: Glutaminase *in situ* activity staining in rat cerebral cortex, hippocampus and cerebellum. Cryostat sections of rat brain (20 μm thick) were subjected to GA activity staining. The formazan production was heterogeneously distributed through hippocampus (A1–A3), cerebral cortex (B1 and B2) and cerebellum (C1 and C2). A1 shows the GA staining in the dentate gyrus with the highest intensity in the granular cell layer (a detailed image in A2 and A3). Cerebral cortex (B1) exhibited GA staining through cortical layers II–VI, and the granular appearance is clearly seen in the neuronal cytoplasm (B2). In the cerebellum (C1), the staining is mainly associated to granular layer and Purkinje cells (see higher magnification in C2). The pattern of staining disappeared when phosphate (D1) or glutamine (D2) were omitted from the reaction mix. M, molecular layer; P, Purkinje cells; G, granular layer of cerebellum; g, dentate gyrus granular layer; h, hilus; mol, dentate gyrus molecular layer. Scale bars 100 μm (C1, B1, A2, D1, and D2); 50 μm (A1, and B2); 25 μm (C2); 20 μm (A3). [Color figure can be viewed in the online issue, which is available at wileyonlinelibrary.com.]**

## Discussion

In this study, we have demonstrated by *in vivo* and *in vitro* approaches that astrocytes express both Gls and Gls2 GA isoforms, so far considered as exclusive neuronal enzymes. The regional expression of GA in rat brain have confirmed and further extended our previous findings dealing with GA in mammalian brain (Olalla et al., 2002), particularly in relation to novel cellular locations and different subcellular localizations shown by Gls and Gls2 isoforms. Of note, this subcellular segregation for GA isoforms was observed in both glutamatergic and GABAergic neuronal populations: the GAB isoform was mostly concentrated in cell nuclei, while KGA appeared in cytoplasm (mitochondria). The same pattern was consistently revealed in rat brain neurons from the main regions examined: cerebral cortex, hippocampus, cerebellum, and striatum. The discovery of GAB in neuronal nuclei of rat and monkey brain represented the first report of an extramitochondrial location for a mammalian GA enzyme (Olalla et al., 2002); in contrast, brain KGA protein was always detected in neuronal mitochondria, in agreement with previous biochemical and immunocytochemical studies (Aoki et al., 1991; Laake et al., 1999; Olalla et al., 2002). Furthermore, in this work novel data support expression of both isoforms in a scarcity of Purkinje cells and in many GABAergic neurons at the molecular layer of the cerebellum, which point toward GA as an important biosynthetic source of Glu at inhibitory synapses indeed, even though early studies did not detect KGA immunoreactivity in GABAergic neurons of neocortex from rodents and monkey (Kaneko et al., 1992; Kaneko and Mitzuno, 1994; Altschuler et al., 1985, 1984; Donoghue et al., 1985). However, more recent studies presented immunocytochemical evidence of the localization of KGA in GABAergic neurons in the cat visual cortex (Van der Gucht et al., 2003) and thalamus (Fisher, 2007), whereby suggesting that Gln can be a metabolic precursor for GABA synthesis. Interestingly, coexpression of KGA and glutamic acid decarboxylase (GAD; EC 4.1.1.15) was also reported in rat hippocampus and basal forebrain neurons (Kaneko and Mitzuno, 1994; Manns et al., 2001).

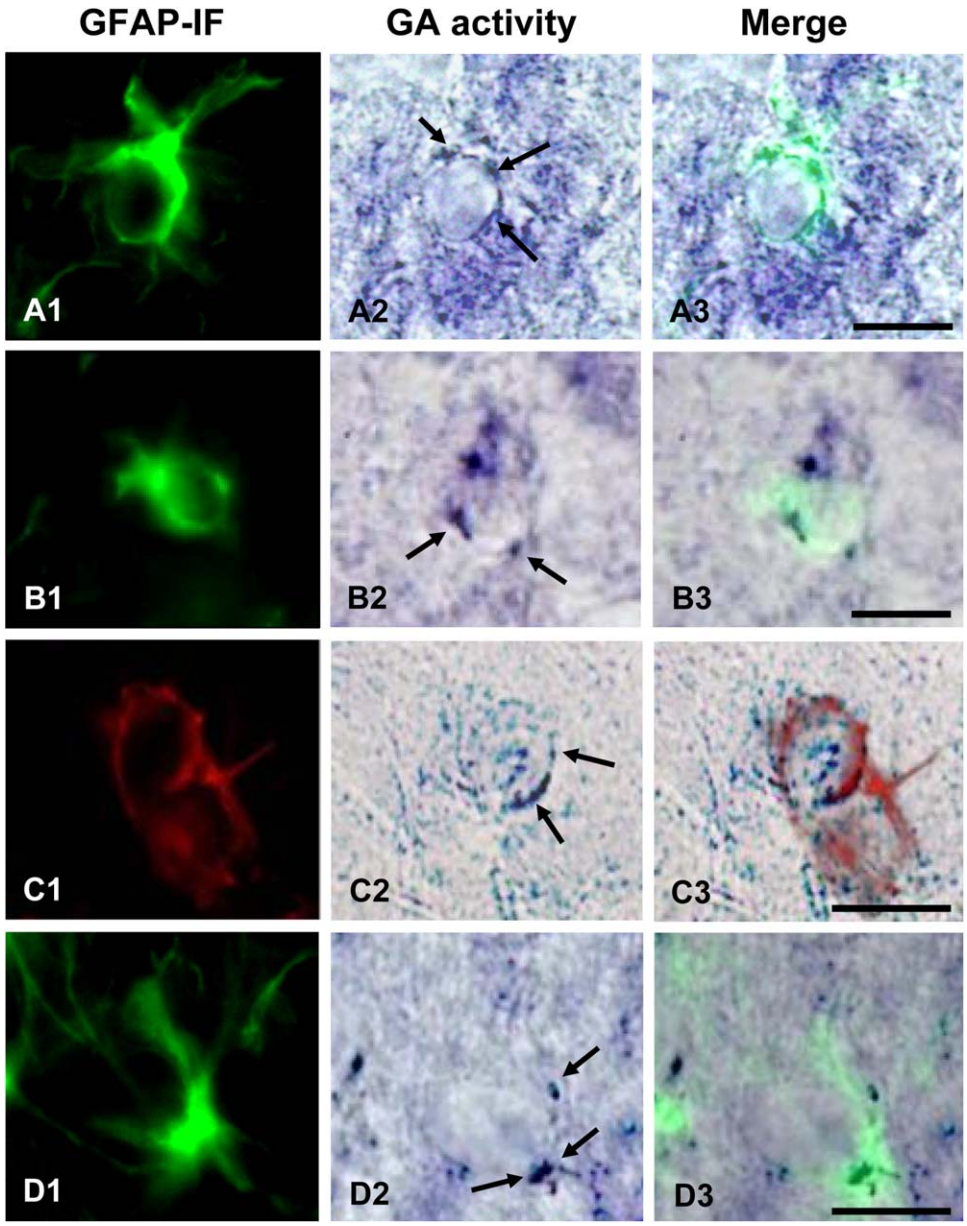


**FIGURE 8: GA activity in rat brain astrocytes. Double labeling in rat brain section (cerebellum, A and D; cortex, B and C) for GFAP (green or red immunofluorescence; A1–D1) and GA activity staining (blue formazan precipitate; A2–D2). Overlapped images (A3–D3) show *in vivo* GA activity as a granular or punctate staining (black arrows) in the cytoplasm of astrocytes. IF, immunofluorescence. Scale bars: 20 μm in all panels. [Color figure can be viewed in the online issue, which is available at wileyonlinelibrary.com.]**

The regional, cellular, and subcellular GA expression in rat brain validated our new set of isoform-specific anti-GA antibodies. Then, we were able to initiate an in-depth study aimed to determine whether astrocytes express functional GA protein isoforms. Contradictory results appear in the literature about the expression of GA in astrocytes: immunohistochemical studies have shown expression of GA protein and GA activity in rat brain astrocytes (Aoki et al., 1991; Wurdig and Kugler, 1991); however, other authors using immunocytochemical techniques reported that GA was not found in astrocytes from human cerebral cortex (Akiyama et al., 1990) and rat cerebellum (Laake et al., 1999). The ultrastructural data obtained by EM for the *Gls*-encoded KGA isoform in rat brain astrocytes indicated that many mitochondria were labeled with a moderate immunostaining, albeit in a significantly lower degree than in neurons. To further characterize the presence of KGA in brain astrocytes, we were impelled to use postmortem human brain tissue, because we did not detect any signal in rat brain astrocytes by immunofluorescence or immunohistochemistry revealed with DAB-Ni. The scarce abundance of KGA protein in astrocytes, and the fact that we were using antibodies against the human enzyme to

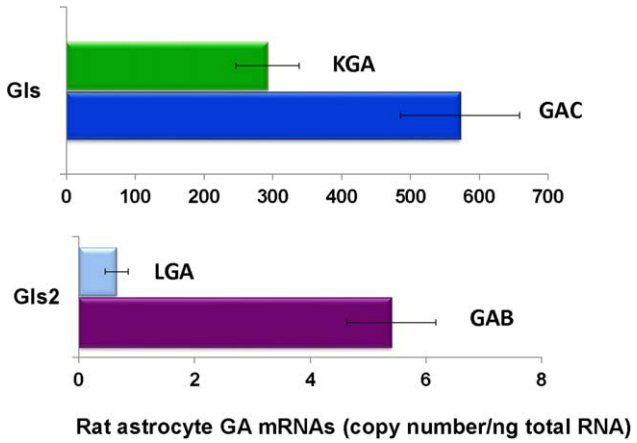


**FIGURE 9: Quantification of mRNA levels of GA transcripts in postnatal cerebellar astrocytes from rat brain by qRT-PCR. The histogram shows the absolute copy number of mRNA transcripts per ng of total RNA for KGA, GAC, GAB, and LGA glutaminase isoforms. Real time RT-PCR was performed as indicated in the Materials and Methods section. Results are mean ± S.E.M. of three independent experiments done in triplicate. [Color figure can be viewed in the online issue, which is available at wileyonlinelibrary.com.]**

recognize the rat KGA isoform, may help to explain this lack of immunoreactivity. However, these problems were overcome by using human brain astrocytes: confocal microscopy of doubly labeled (KGA/GFAP) astrocytes from temporal cortex revealed a strong immunoreactivity in many cells with a granular or punctate shape typical of mitochondria. Accordingly, the distribution of KGA in cultured astrocytes fully mimics that of the mitochondrial marker ATP synthase, reinforcing the view that this Gls isoform is located in astrocyte mitochondria, the same subcellular location shown by KGA in neurons (Olalla et al., 2002).

Identification of the existence of GA isoforms in astrocytes is of great importance to fully understand the bioenergetics of glial cells and, particularly, to shed light into transmitter recycling and short-term regulation of the Glu/Gln cycle which takes place between neurons and astrocytes (Hertz, 1979; Berl and Clarke, 1983). The Glu released by neurons is taken up by nearby astrocytes at the synaptic cleft through efficient Glu transport systems and then converted to Gln by glutamine synthetase (GS; EC 6.3.1.2), an enzyme exclusively located in astrocytes (Norenberg and Martínez-Hernández, 1979). The Glu-derived Gln is finally exported back to neurons where GA generates neurotransmitter Glu. The cycle is a key mechanism for homeostatic control of Glu, Gln, and GABA concentrations; however, it is not always a stoichiometric pathway because part of the exogenous Glu taken by astrocytes does not end as Gln but used to fulfill other energy and metabolic purposes instead (Sonnewald et al., 1993). Actually, it has been estimated that 10%–30% of synaptic-derived Glu is oxidized by astrocytes and must be replenished to keep the carbon balance of the Glu/Gln cycle. *In vivo* studies, using $^{13}$C-NMR spectroscopy, indicated that glial anaplerosis from glucose, through the astrocyte-specific enzyme pyruvate carboxylase (PC; EC 6.4.1.1) is the main contributor for replacing the oxidatively degraded Glu (Rothman et al., 1999; Lebon et al., 2002).

While the functional significance of GA in astrocytes is not completely known, at least three advantages can be envisioned, particularly in periods of intense synaptic activity. First, functional GA activity will endorse astrocytes with a mitochondrial source of Glu (and ammonium) whilst its synthesis from Gln does not require energy. Catabolism of this endogenous Gln-derived Glu may cooperate with the strong energy and biosynthetic needs required by astrocytes, thus preserving most of the exogenous synaptic Glu to be transformed back to Gln and redirected toward neurons. In this way, astrocytes will not significantly deplete synaptic Glu stores saving most of it for Gln synthesis in the cytosol; such mechanism might be particularly relevant in periods of great synaptic activity. In addition, the ammonium generated in mitochondria by this glutaminolytic process could be channeled to Gln synthesis in cytosol, providing an additional source of nitrogen needed to recycle Glu in Gln. Furthermore, the fast induction of GS protein in active synapse, which may rapidly convert the captured synaptic Glu into Gln, means that the flux of Glu to the TCA cycle became negligible as compared with the flux through GS (Fonseca et al., 2005): under these conditions, the supply of endogenous Glu by GA would be highly valuable for astrocyte bioenergetics.

Second, a GA activity will increase the metabolic versatility of astrocytes in such way that they do not have to exclusively rely on PC for *de novo* synthesis of Glu. The existence of a functional astrocyte GA will diminish the anaplerotic pressure, which is important because Glu synthesis by anaplerosis would be detrimental if it is not matched by degradation through cataplerotic routes (Sonnewald, 2014). And third, *in situ* generation of mitochondrial Glu avoids another problem faced by synaptic cytosolic Glu: its import into astrocytic mitochondria. It has been shown that brain astrocytes do not express the main aspartate-glutamate carrier (*Aralar/AGC1*) (Ramos et al., 2003; Berckich et al., 2007); therefore, exogenous Glu must enter into astrocytes uniquely by the Glu/hydroxyl carrier. However, results obtained from KO mice for *Aralar* underscored the importance of this carrier for Glu transport in brain and skeletal muscle mitochondria (Jalil et al., 2005), and further evidences indicate that no other Glu carrier can substitute for *Aralar* in those tissues (Satrústegui et al., 2007 and references therein). In contrast, Gln can be actively concentrated into astrocyte mitochondria using a high-affinity mitochondrial Gln carrier (Roberg et al., 1999),

and then be released into the mitochondrial matrix near the GA catalytic site (Matés et al., 2009). The generation of Glu into the matrix facilitates their further catabolism for bioenergetic or biosynthetic purposes. Thus, Gln-derived Glu is generated into the mitochondrial matrix without the need of an additional carrier, as required for exogenous Glu. Finally, it should be emphasized that astrocyte GA might have physiological sense spatially confined to the mitochondria; a cytosolic activity seems unlikely taking into account the strong inhibition that synaptic Glu may exert on GA activity. In addition, the simultaneous operation of GA and GS in the cytosol will give rise to a futile cycle with high energy expenditure in the form of ATP.

In addition to physiological role of GA in astrocytes as noted above, presence of GA in astrocytic mitochondria may exert detrimental effects in these cells under certain pathological conditions associated with acute hepatic encephalopathy (HE), wherein increased astrocytic levels of Gln is a characteristic feature (Albrecht and Norenberg, 2006; Rama Rao and Norenberg, 2014). Such increased astrocytic levels of Gln results from excessive conversion of ammonia (accumulated in large amounts in brain due to the inability of diseased liver to detoxify gut-derived nitrogenous material) to Gln, a process mediated by GS, which is predominantly present in astrocytes (Norenberg and Martinez-Hernandez, 1979). It has recently been proposed that excess Gln present in astrocytes in acute HE will be transported into mitochondria where it is converted to ammonia and Glu, a process mediated by GA, and such increased ammonia levels in the astrocytic mitochondria were shown to be responsible for many of pathogenetic events in acute HE (e.g., oxidative/nitrative stress, mitochondrial permeability transition), the so called "Trojan horse hypothesis," ultimately leading to astrocyte dysfunction (Albrecht and Norenberg, 2006; Rama Rao and Norenberg, 2014). Therefore, the presence of GA in the mitochondria of astrocytes is not only physiologically significant, but could be also detrimental in neurological disorders associated with excessive accumulation of Gln.

The co-existence of several GA isoforms in single cells has been also related to novel functions that these proteins may accomplish in brain; for example, the nuclear localization reported for the GAB isoform in neurons (Olalla et al., 2002) and astrocytes (this work). GAB was mostly concentrated in neuronal nuclei, although a minor cytoplasmic immunolabeling was also detected. With regard to this issue, we previously reported cytoplasmic expression of GAB in astrocytic cell body and processes (including perivascular end feet) which co-localizes with the PDZ protein GIP ("Glutaminase-Interacting Protein") (Olalla et al., 2008). The mitochondrial location of KGA and GAB in astrocytes may be a control mechanism allowing broad and fine tuning of Glu production depending on their energetic needs and/or synaptic activity. In this context, it is noteworthy the significant increase in mitochondrial GAB detected in cultured astrocytes, using a standard culture medium containing Gln, compared with the scarce mitochondrial label observed in rat brain tissue. This fact easily illustrates how astrocytes can modulate expression of GA isoforms, depending on the environmental conditions to which are they exposed, to maintain their energy and metabolic homeostasis. Mammalian KGA and GAB proteins possess different kinetic and regulatory properties; therefore, they reach full catalytic activity at different cellular concentrations of Gln, Glu, and Pi (Márquez et al., 2010). In this work, we have shown functional GA activity in the cytoplasm of discrete populations of hippocampal and cerebellar astrocytes, which can be ascribed to mitochondrial GA. In contrast, no activity was revealed in astrocytic nuclei. However, this result may arise because our NBT-based activity assay was not sensitive enough for very low activity levels in nucleus. In fact, nuclear fractions isolated from rat brain showed GA activity although with kinetic properties distinct from classical *Gls2*-encoded LGA isoform (Olalla et al., 2002). Interestingly, purified human GAB isozyme showed mixed kinetic characteristics of K- and L-type isoforms (Campos-Sandoval et al., 2007) in accord with the results obtained from nuclear rat brain extracts. The existence of GA activity *in vivo* in astrocytes had not yet been proved. Primary cultures of astrocytes displayed strong GA activity (Schousboe et al., 1979; Kvamme et al., 1982; Yudkoff et al., 1988) and GA mRNA transcripts (Szeliga et al., 2008), but these *in vitro* results were questioned arguing that GA could be induced by the culture conditions (Erecinska and Silver, 1990).

The significance of the nuclear location of GAB in neurons and astrocytes remains to be fully determined. However, it has been related with transcriptional regulation associated to differentiation (Olalla et al., 2002; Márquez et al., 2006). In this regard, a recent study has revealed that overexpression of human GAB in T98G glioblastoma cell line induced a marked reversion of their transformed phenotype, along with a massive change in cell's transcriptome linked to a potential function of GAB as transcriptional coregulator (Szeliga et al., 2009), but the concrete molecular mechanisms underlying this phenotypical change are still unknown. Interestingly, recent experimental evidences obtained from *in vitro* cultures of mouse embryonary cortical neurons support our hypothesis relating Gls2 with cell differentiation: inhibition of GA activity blocked *in vitro* differentiation of these neurons and *in vivo* Gls2 expression was significantly enhanced during postnatal development of mouse cerebellum, particularly at the P1 to P8 interval characterized by a massive expansion of granule cell progenitors (Velletri et al., 2013).

Our study on GA expression in astrocytes was completed with the quantification of the absolute mRNA levels of GA transcript variants using isoform-specific qRT-PCR. We performed the analysis in rat cerebellum because this region showed a high number of positive astrocytes for the *in situ* activity staining. We found that all four GA isoforms were transcribed in astrocytes, although with marked differences in their expression values. In accordance with the results obtained at the protein level, the Gls-encoded transcripts showed an overwhelming abundance in cerebellar postnatal astrocytes compared with the scarce level of Gls2 transcripts. This result agrees with our previous quantification of whole brain GA mRNA levels in mammals, where Gls were the predominant isoenzymes accounting for more than 90% of total GA transcripts (Martín-Rufián et al., 2012). Surprisingly, in rat postnatal cerebellar astrocytes the alternatively spliced GAC mRNA levels were even higher than those obtained for KGA. With regard to Gls2 transcripts, GAB showed the greatest abundance in astrocytes versus LGA, in full agreement with previous results obtained by qRT-PCR of rat total brain (Martín-Rufián et al., 2012).

In conclusion, GABAergic neurons and astrocytes express Gls and Gls2 isoenzymes in nucleus and mitochondria, in addition to glutamatergic neurons. Therefore, GA is no longer a reliable neurochemical marker of glutamatergic neurons and synapses. Astroglial cells are capable of generating Glu from Gln through GA pathway. Further studies are needed to elucidate the physiological roles of these two isoforms, the molecular mechanisms controlling their reciprocal expression in brain tissue and the relative contributions of each isozyme to the generation of metabolic and neurotransmitter pools of Glu. It remains also to be determined whether inhibition of GA activity/function in mitochondria or nucleus may contribute to glial cell dysfunction with pathological consequences.

## Acknowledgment

Grant sponsor: Regional Government of Andalusia; Grant numbers: CVI-6656; CTS-2035; Grant sponsor: RTA RETICS Network from the Spanish Health Institute Carlos III; Grant number: RD06/1012; Grant sponsor: FIS; Grant numbers: PI12/01439; PI12/01431; Grant sponsor: CIBERNED; Grant number: PI2013/01

The expert technical assistance of Laura Castilla is gratefully acknowledged. No potential conflicts of interest were disclosed.

## References

Akiyama H, Kaneko T, Mizuno N, McGeer PL. 1990. Distribution of phosphate-activated glutaminase in the human cerebral cortex. J Comp Neurol 297:239–252.

Albrecht J, Norenberg MD. 2006. Glutamine: A Trojan horse in ammonia neurotoxicity. Hepatology 44:788–794.

Aledo JC, Gómez-Biedma S, Segura JA, Molina M, Núñez de Castro I, Márquez J. 1993. Native polyacrylamide gel electrophoresis of membrane proteins: Glutaminase detection after in situ specific activity staining. Electrophoresis 14:88–93.

Aledo JC, Gómez-Fabre PM, Olalla L, Márquez J. 2000. Identification of two human glutaminase loci and tissue-specific expression of the two related genes. Mamm Genome 11:1107–1110.

Altschuler RA, Wenthold RJ, Schwartz AM, Haser WG, Curthoys NP, Parakkal MH, Fex J. 1984. Immunocytochemical localization of glutaminase-like immunoreactivity in the auditory nerve. Brain Res 291:173–178.

Altschuler RA, Monaghan DT, Haser WG, Wenthold RJ, Curthoys NP, Cotman CW. 1985. Immunocytochemical localization of glutaminase-like and aspartate aminotransferase-like immunoreactivities in the rat and guinea pig hippocampus. Brain Res 330:225–233.

Alvarez-Buylla A, Garcia-Verdugo JM, Tramontin AD. 2001. A unified hypothesis on the lineage of neural stem cells. Nat Rev Neurosci 2:287–293.

Aoki C, Kaneko T, Starr A, Pickel VM. 1991. Identification of mitochondrial and non-mitochondrial glutaminase within select neurons and glia of rat forebrain by electron microscopic immunocytochemistry. J Neurosci Res 28:531–548.

Araque A, Parpura V, Sanzgiri RP, Haydon PG. 1998. Glutamate-dependent astrocyte modulation of synaptic transmission between cultured hippocampal neurons. Eur J Neurosci 10:2129–2142.

Araque A, Parpura V, Sanzgiri RP, Haydon PG. 1999. Tripartite synapses: Glia, the unacknowledged partner. Trends Neurosci 22:208–215.

Araque A, Li N, Doyle RT, Haydon PG. 2000. SNARE protein-dependent glutamate release from astrocytes. J Neurosci 20:666–673.

Attwell D, Buchan AM, Charpak S, Lauritzen M, MacVicar BA, Newman EA. 2010. Glial and neuronal control of brain blood flow. Nature 468:232–243.

Auld DS, Robitaille R. 2003. Glial cells and neurotransmission: An inclusive view of synaptic function. Neuron 40:389–400.

Barcia C Sr, Mitxitorena I, Carrillo-de Sauvage MA, Gallego JM, Pérez-Vallés A, Barcia C Jr. 2013. Imaging the microanatomy of astrocyte-T-cell interactions in immune-mediated inflammation. Front Cell Neurosci 7:1–10.

Berckich DA, Ola MS, Cole J, Sweatt, AJ, Hutson SM. 2007. Mitochondrial transport proteins of the brain. J Neurosci Res 85:3367–3377.

Berl S, Clarke DD. 1983. The metabolic compartmentation concept. In: Hertz L, Kvamme E, McGeer EG, Schousboe A, editors. Glutamine, glutamate and GABA in the central nervous system. New York: Alan R. Liss, Inc. pp 205–217.

Campos JA, Aledo JC, Segura JA, Alonso FJ, Gómez-Fabre PM, Núñez de Castro I, Márquez J. 2003. Expression of recombinant human L-glutaminase in *Escherichia coli*: Polyclonal antibodies production and immunological analysis of mouse tissues. Biochim Biophys Acta 1648:17–23.

Campos-Sandoval JA, López de la Oliva AR, Lobo C, Segura JA, Matés JM, Alonso FJ, Márquez J. 2007. Expression of functional human glutaminase in baculovirus system: Affinity purification, kinetic and molecular characterization. Int J Biochem Cell Biol 39:765–773.

Curthoys NP, Watford M. 1995. Regulation of glutaminase activity and glutamine metabolism. Annu Rev Nutr 15:133–159.

Danbolt NC. 2001. Glutamate uptake. Prog Neurobiol 65:1–105.

de la Rosa V, Campos-Sandoval JA, Martín-Rufián M, Cardona C, Matés JM, Segura JA, Alonso FJ, Márquez J. 2009. A novel glutaminase isoform in mammalian tissues. Neurochem Int 55:76–84.

Donoghue JP, Wenthold RJ, Altschuler RA. 1985. Localization of glutaminase-like and aspartate aminotransferase-like immunoreactivity in neurons of cerebral neocortex. J Neurosci 5:2597–2608.

Elgadi KM, Meguid RA, Qian M, Souba WW, Abcouwer SF. 1999. Cloning and analysis of unique human glutaminase isoforms generated by tissue-specific alternative splicing. Physiol Genomics 1:51–62.

Erecinska M, Silver IA. 1990. Metabolism and role of glutamate in mammalian brain. Prog Neurobiol 35:245–296.

Fisher RS. 2007. Co-localization of glutamic acid decarboxylase and phosphate-activated glutaminase in neurons of lateral reticular nucleus in feline thalamus. Neurochem Res 32:177–186.

Fonseca LL, Monteiro MAR, Alves PM, Carrondo MJT, Santos H. 2005. Cultures of rat astrocytes challenged with a steady supply of glutamate: New model to study flux distribution in the glutamate-glutamine cycle. Glia 51: 286–296.

Gómez-Fabre PM, Aledo JC, del Castillo-Olivares A, Alonso FJ, Núñez de Castro I, Campos JA, Márquez J. 2000. Molecular cloning, sequencing and expression studies of the human breast cancer cell glutaminase. Biochem J 345:365–375.

Hertz L. 1979. Functional interactions between neurons and astrocytes. I. Turnover and metabolism of putative amino acid transmitters. Prog Neurobiol 13:277–323.

Hertz L. 2004. Intercellular metabolic compartmentation in the brain: Past, present and future. Neurochem Int 45:285–296.

Iliff JJ, Lee H, Yu M, Feng T, Logan J, Nedergaard M, Benveniste H. 2013. Brain-wide pathway for waste clearance captured by contrast-enhanced MRI. J Clin Invest 123:1299–1309.

Jalil MA, Begum L, Contreras L, Pardo B, Iijima M, Li MX, Ramos M, Marmol P, Horiuchi M, Shimotsu K, Nakagawa S, Okubo A, Sameshima M, Isashiki Y, del Arco A, Kobayashi K, Satrústegui J, Saheki T. 2005. Reduced N-acetylaspartate levels in mice lacking aralar, a brain- and muscle-type mitochondrial aspartate-glutamate carrier. J Biol Chem 280:31333–31339.

Jayakumar AR, Tong XY, Curtis KM, Ruiz-Cordero R, Shamaladevi N, Abuzamel M, Johnstone J, Gaidosh G, Rama Rao KV, Norenberg MD. 2014. Decreased astrocytic thrombospondin-1 secretion after chronic ammonia treatment reduces the level of synaptic proteins: in vitro and in vivo studies. J Neurochem, doi: 10.1111/jnc.12810.

Kaneko T, Mizuno N. 1994. Glutamate-synthesizing enzymes in GABAergic neurons of the neocortex: A double immunofluorescence study in the rat. Neuroscience 61:839–849.

Kaneko T, Nakaya Y, Mizuno N. 1992. Paucity of glutaminase-immunoreactive non-pyramidal neurons in the rat cerebral cortex. J Comp Neurol 322:181–190.

Kvamme E, Svenneby G, Hertz L, Schousboe A. 1982. Properties of phosphate activated glutaminase in astrocytes cultured from mouse brain. Neurochem Res 7:761–770.

Laake JH, Takumi Y, Eidet J, Torgner IA, Roberg B, Kvamme E, Ottersen OP. 1999. Postembedding immunogold labelling reveals subcellular localization and pathway-specific enrichment of phosphate activated glutaminase in rat cerebellum. Neuroscience 88:1137–1151.

Lebon V, Petersen KF, Cline GW, Shen J, Mason GF, Dufour S, Behar KL, Shulman GI, Rothman DL. 2002. Astroglial contribution to brain energy metabolism in humans revealed by $^{13}C$ nuclear magnetic resonance spectroscopy: Elucidation of the dominant pathway for neurotransmitter glutamate repletion and measurement of astrocytic oxidative metabolism. J Neurosci 22:1523–1531.

Magistretti PJ. 2006. Neuron-glia metabolic coupling and plasticity. J Exp Biol 209:2304–2311.

Manns ID, Mainville L, Jones BE. 2001. Evidence for glutamate, in addition to acetylcholine and GABA, neurotransmitter synthesis in basal forebrain neurons projecting to the entorhinal cortex. Neuroscience 107:249–263.

Márquez J, López de la Oliva AR, Matés JM, Segura JA, Alonso FJ. 2006. Glutaminase: A multifaceted protein not only involved in generating glutamate. Neurochem Int 48:465–471.

Márquez J, Matés JM, Segura JA, Campos-Sandoval JA, Lobo C, Alonso FJ. 2010. Brain glutaminases. Biomol Concepts 1:3–15.

Martín-Rufián M, Tosina M, Campos-Sandoval JA, Manzanares E, Lobo C, Segura JA, Alonso FJ, Matés JM, Márquez J. 2012. Mammalian glutaminase Gls2 gene encodes two functional alternative transcripts by a surrogate promoter usage mechanism. PLoS ONE 7:e38380.

Martín-Rufián M, Nascimento-Gomes R, Higuero A, Crisma AR, Campos-Sandoval JA, Gómez-García MC, Cardona C, Cheng T, Lobo C, Segura JA, Alonso FJ, Szeliga M, Albrecht J, Curi R, Márquez J, Colquhoun A, Deberardinis RJ, Matés JM. 2014. Both GLS silencing and GLS2 overexpression synergize with oxidative stress against proliferation of glioma cells. J Mol Med 92:277–290.

Matés JM, Segura JA, Campos-Sandoval JA, Lobo C, Alonso L, Alonso, FJ, Márquez J. 2009. Glutamine homeostasis and mitochondrial dynamics. Int J Biochem Cell Biol 41:2051–2061.

Matés JM, Segura JA, Martín-Rufián M, Campos-Sandoval JA, Alonso FJ, Márquez J. 2013. Glutaminase isoenzymes as key regulators in metabolic and oxidative stress against cancer. Curr Mol Med 13:514–534.

Montero F, Baglietto-Vargas D, Moreno-González I, López-Tellez JF, Cuesta-Munoz AL, Gutiérrez A, Aledo JC. 2007. Glutaminase activity is confined to the mantle of the islets of Langerhans. Biochimie 89:1366–1371.

Nicklas WJ, Zeevalk G, Hyndman A. 1987. Interactions between neurons and glia in glutamate/glutamine compartmentation. Biochem Soc Trans 15:208–210.

Norenberg MD, Martínez-Hernández A. 1979. Fine structural localization of glutamine synthetase in astrocytes of rat brain. Brain Res 161:303–310.

Olalla L, Gutiérrez A, Campos JA, Khan ZU, Alonso F, Segura JA, Márquez, J, Aledo JC. 2002. Nuclear localization of L-glutaminase in mammalian brain. J Biol Chem 277:38939–38944.

Olalla L, Gutiérrez A, Jiménez AJ, López-Téllez JF, Khan ZU, Pérez J, Alonso FJ, de la Rosa V, Campos-Sandoval JA, Segura JA, Aledo JC, Márquez J. 2008. Expression of scaffolding PDZ protein GIP (Glutaminase-Interacting-Protein) in mammalian brain. J Neurosci Res 86:281–292.

Pellerin L, Magistretti P. 1994. Glutamate uptake into astrocytes stimulates aerobic glycolisis: A mechanism coupling neuronal activity to glucose utilization. Proc Natl Acad Sci USA 91:10625–10629.

Perea G, Navarrete M, Araque A. 2009. Tripartite synapses: Astrocytes process and control synaptic information. Trends Neurosci 32:421–431.

Porter LD, Ibrahim H, Taylor L, Curthoys NP. 2002. Complexity and species variation of the kidney-type glutaminase gene. Physiol Genomics 9:57–66.

Rama Rao KV, Norenberg MD. 2014. Glutamine in the pathogenesis of hepatic encephalopathy: The trojan horse hypothesis revisited. Neurochem Res 39:593–598.

Ramos M, del Arco A, Pardo B, Martínez-Serrano A, Martínez-Morales JR, Kobayashi K, Yasuda T, Bogonez E, Bovolenta P, Saheki T, Satrústegui J. 2003. Developmental changes in the $Ca^{2+}$-regulated mitochondrial aspartate-glutamate carrier aralar1 in brain and prominent expression in the spinal cord. Dev Brain Res 143:33–46.

Roberg B, Torgner IA, Kvamme E. 1999. Inhibition of glutamine transport in rat brain mitochondria by some amino acids and tricarboxylic acid cycle intermediates. Neurochem Res 24:811–816.

Rothman DL, Sibson NR, Hyder F, Shen J, Behar KL, Shulman RG. 1999. In vivo nuclear magnetic resonance spectroscopy studies of the relationship between the glutamate-glutamine neurotransmitter cycle and functional neuroenergetics. Philos Trans R Soc Lond B 354:1165–1177.

Satrústegui J, Contreras L, Ramos M, Marmol P, del Arco A, Saheki T, Pardo P. 2007. Role of aralar, the mitochondrial transporter of aspartate-glutamate, in brain N-acetylaspartate formation and $Ca^{2+}$ signaling in neuronal mitochondria. J Neurosci Res 85:3359–3366.

Saura J, Tusell JM, Serratosa J. 2003. High-yield isolation of murine microglia by mild trypsinization. Glia 44:183–199.

Schousboe A, Hertz L, Svenneby G, Kvamme E. 1979. Phosphate activated glutaminase activity and glutamine uptake in primary cultures of astrocytes. J Neurochem 32:943–950.

Sonnewald U. 2014. Glutamate synthesis has to be matched by its degradation: Where do all the carbons go? J Neurochem (Jul 2). doi:10.1111/jnc.12812. [Epub ahead of print].

Sonnewald U, Westergaard N, Petersen SB, Unsgard G, Schousboe A. 1993. Metabolism of [U-13C]glutamate in astrocytes studied by 13C NMR

spectroscopy: Incorporation of more label into lactate than into glutamine demonstrates the importance of the tricarboxylic acid cycle. J Neurochem 61:1179–1182.

Szeliga M, Matyja E, Obara M, Grajkowska W, Czernicki T, Albrecht J. 2008. Relative expression of mRNAs coding for glutaminase isoforms in CNS tissues and CNS tumors. Neurochem Res 33:808–813.

Szeliga M, Obara-Michlewska M, Matyja E, Lazarczyk M, Lobo C, Hilgier W, Alonso F, Márquez J, Albrecht J. 2009. Transfection with liver-type glutaminase (LGA) cDNA alteres gene expression and reduces viability, migration and proliferation of T98G glioma cells. Glia 57:1014–1023.

Takeuchi H, Jin S, Wang J, Zhang G, Kawanokuchi J, Kuno R, Sonobe Y, Mizuno T, Suzumura A. 2006. Tumor necrosis factor-α induces neurotoxicity via glutamate release from hemichannels of activated microglia in an autocrine manner. J Biol Chem 281:21362–21368.

Van der Gucht E, Jacobs S, Kaneko T, Vandesande F, Arckens L. 2003. Distribution and morphological characterization of phosphate-activated glutaminase-immunoreactive neurons in cat visual cortex. Brain Res 988:29–42.

Velletri T, Romeo F, Tucci P, Peschiaroli A, Annicchiarico-Petruzzelli M, Niklison-Chirou MV, Amelio I, Knight RA, Mak TW, Melino G, Agostini M. 2013. GLS2 is transcriptionally regulated by p73 and contributes to neuronal differentiation. Cell Cycle 12:1–10.

Verkhratsky A, Sofroniew MV, Messing A, deLanerolle NC, Rempe D, Rodríguez JJ, Nedergaard M. 2012. Neurological diseases as primary gliopathies: A reassessment of neurocentrism. ASN Neuro 4:131–148.

Wurdig S, Kugler P. 1991. Histochemistry of glutamate metabolizing enzymes in the rat cerebellar cortex. Neurosci Lett 130:165–168.

Yudkoff M, Nissim I, Pleasure D. 1988. Astrocyte metabolism of [$^{15}$N]glutamine: Implications for the glutamine-glutamate cycle. J Neurochem 51:843–850.